MEASURING COLLISIONAL RELAXATION IN CLUSTERS FROM PHOTOFRAGMENT ANGLE-VELOCITY DISTRIBUTIONS

Jack A. Syage

The Aerospace Corporation, P.O. Box 92957,
M5-754, Los Angeles, CA 90009

ABSTRACT

The photodissociation of molecules in clusters affords the opportunity to study collisional relaxation of translational and rovibrational energy under solvent-like conditions. We have measured the angle-velocity distribution of $I(^2P_{3/2})$ and $I(^2P_{1/2})$ from photodissociation of $(CH_3I)_n$ clusters at 266 and 304 nm. For monomer (n=1), the angular distributions are very anisotropic and the translational energy is sharply peaked at high energy. For clusters (predominantly n=2,3), the I atom undergoes collisions, which substantially relax the translational energy and anisotropy. We have measured an anisotropy that increases with increasing translational energy. This observation is believed to reflect the correlation of anisotropy and energy loss due to the residence time and number of collisions of the photofragment in the cluster. Anisotropy vs translational energy plots may be interpreted to give collisional relaxation rates in clusters.

INTRODUCTION

Research in clusters holds the potential to learn about condensed-phase properties at the single-molecule state-to-state level. Our interest has mostly focussed on time-domain measurements of chemically reacting systems.[1] In this work, we take a different approach toward measuring fast dynamics in clusters. Here we are interested in measuring collisional relaxation of translational, vibrational, and rotational energy in clusters. The method is based on photodissociating a molecule in a cluster and measuring the change in the nascent rovibrational and translational energy of the fragment due to collisions within the cluster. However, rather than time-resolve these properties within the cluster, we instead probe the energy distributions of the fragments that escape the cluster. What is needed is a method to determine how much time a fragment has spent in the cluster before escaping. This can be achieved using an ultrafast pump-probe sequence for cluster photodissociation and photofragment detection. We plan to initiate such experiments. However, ultrafast pulses do not enable one to measure photofragment energy distributions at high resolution due to the large frequency bandwidth of the short pulses. In this work we use narrow band nanosecond pulses to measure the fragment energy distribution and rely on the anisotropy of the fragments as a measure of the residence time of the fragment in the cluster.

Spectroscopic studies of reaction products from van der Waals molecules were introduced by Soep, Jouvet, and coworkers[2] and Wittig and coworkers[3,4] (we distinguish this chemistry from the more extensive studies of van der Waals dissociation). These investigators measured product rovibrational distributions for prealigned collision parameters. State-specific detection of product has recently been extended into the femtosecond domain by the groups of Zewail[5] and Wittig[4].

The measure of product translational energy from photoinitiated cluster reactions is emerging as a powerful tool. Many of these studies have focussed on cluster ion photodissociation.[6] Studies of neutral cluster photodissociation require a photofragment probe pulse (e.g., for ionization); however, this enables state-specific detection. Wittig has recently implemented a method for measuring high resolution translational energy spectra of H atoms scattering out of complexes by exciting them to high n Rydberg states, which then field ionize at the detector.[7] The Miller group has applied the novel use of a strong electric fields to orient complexes such as N_2-HF for angle-resolved measurements.[8] In studies of CH_3I monomer photodissociation, Ogorzalek Loo *et al* [9] and Penn *et al* [10] and observed that cluster formation broadens the time-of-flight spectrum for I atom. The monomer dissociation is known to be very anisotropic with a velocity distribution sharply peaked at high energy. The product velocity distribution for the clusters, however, was broad and peaked at zero component-velocity.

In the present work, we recorded the angular dependence of the I atom velocity distribution in the $^2P_{3/2}$ and $^2P_{1/2}$ state (henceforth I and I*) following excitation of $(CH_3I)_n$ (n=1-3) at 266 and 304 nm. As noted by Ogorzalek Loo *et al* [9] and Penn *et al*[10] above, the results are remarkably different from that recorded for photodissociation of the isolated molecule CH_3I. We have measured the angle-dependent translational energy distribution and product branching ratio I/I*. Young has recently measured I atom and H atom translational energy spectra for $(HI)_n$ cluster photodissociation.[11]

EXPERIMENTAL

Our experiments are conducted in a molecular beam time-of-flight (TOF) mass spectrometer.[12,13] The TOF mass spectrometer consists of an ion optics assembly of three grids separated by 1 cm, a one-meter drift tube, and a 5-mm-diam aperture mounted in front of an 18-mm diam microchannel plate detector. The results presented here were collected using 30 V/cm and 480 V/cm for the extraction and acceleration fields, respectively. Under these operating conditions, I^+ ions have flight times centered at t_0 = 42 μs. The detection geometry for measuring angle-resolved TOF spectra is explained elsewhere.[13] The fragment 3-dimensional spatial distribution expands as it travels down the drift tube to the detector. An aperture placed in front of the detector limits the field-of-view to a cylinder of ions of maximum radial velocity $v_r = r/t_0$ where r is the effective aperture radius, and t_0 is the ion packet drift

time. The angular and energy resolutions are dependent on photofragment speed v and are given by

$$\Delta\theta_z = \arcsin(v_r/v) \qquad \text{(angular resolution)} \qquad (1)$$

$$\Delta v = 1 - (v_{z,min}/v) = 1 - \cos\Delta\theta_z \qquad \text{(energy resolution)} \qquad (2)$$

The detection cylinder limits the range of v_z corresponding to a particular v, which defines Δv. As v_r decreases relative to v, the detected v_z distribution becomes a good measure of the speed distribution v. In the present work, we probe through the center of the ion 3D velocity distribution at different angles α relative to the laser polarization axis ε. In previous work, we recorded series of 1D TOF spectra by sequentially offsetting the detection cylinder from centerline, thereby mapping out a 2D section of the 3D velocity distribution.[12]

Photolysis was initiated at 266 nm or 304 nm. I and I* photofragment were ionized by 2+1 resonance enhanced multiphoton ionization (REMPI) using excitation at 304.7 nm ($^6P^2D^0_{5/2}$ intermediate state) and 304.0 nm ($^6P^4D^0_{1/2}$ state), respectively. For 266-nm photolysis, the pump pulse precedes the probe pulse by about 10 ns. For 304-nm photolysis, the pump and probe pulses are the same. The laser polarization angle α of the pump was varied by rotating a combination of a double Fresnel-Rhomb and a Glan-Taylor polarizer. Flat windows were used on the molecular beam port to minimize polarization dependent transmission. The incident pump and probe laser pulse energies were measured using a photodiode at the exit window of the molecular beam. Laser pulse energies and focussing conditions were adjusted to avoid space charge repulsion and in the case of 266-nm photolysis to maximize the two-pulse signal relative to the one-color signal. TOF spectra were collected using a LeCroy 9450 digital scope.

The CH_3I sample was placed in a bubbler cooled to 0°C and delivered to the pulsed valve by a flow of Ar at 1000 Torr (results were unchanged at lower temperatures). To reduce cluster formation, the pulsed valve was heated to 60°C. Near cluster-free monomer TOF spectra could be obtained by synchronizing laser excitation to the leading edge of the gas pulse. Increasing amounts of cluster signal could be obtained by moving the laser excitation toward the peak of the gas pulse.

RESULTS AND DISCUSSION

Observed TOF traces $I_0(v_z)$ and $I_{90}(v_z)$ for 0 and 90° photofragment recoil angles are presented in Fig. 1 for the detection of the $I(^2P_{3/2})$ photofragment from 266-nm photolysis of $(CH_3I)_n$ monomers and clusters. The series of figures 1a,a' to 1c,c' represent conditions of increasing clustering. Calculated curves are fitted to the data. The curve fits to the monomer results were calculated from the known velocity distribution $g(v)$ recorded at higher resolution and the instrument function corresponding to the present experiment. The curve fits to the cluster results were calculated from a single Gaussian function. The following observations are evident in Fig. 1.

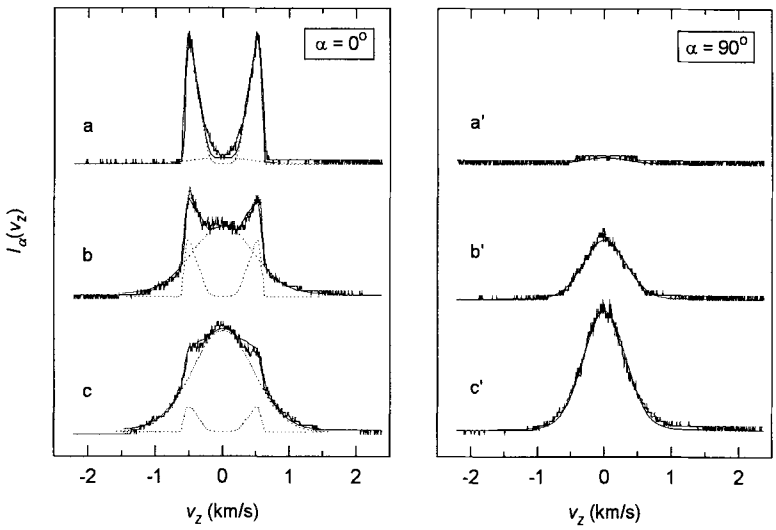

FIG 1. Angle-resolved I($^2P_{3/2}$) photofragment velocity distributions $I_\alpha(v_z)$ for $(CH_3I)_n$ excitation at 266 nm where α is the alignment of ε relative to the drift tube *z*-axis and θ = α is the product recoil angle relative to ε. (a,a') monomer excitation, (b,b') monomer and cluster excitation, (c,c') increasing cluster distribution. Calculated fits are shown (—) along with the individual contributions due to monomer and cluster excitation (····).The calculated $I_\alpha(v_z)$ spectra were fitted to Gaussian functions (—) of the form $\exp\{-v_z^2/\sigma_v^2\}$ where σ_v^2 is 0.65 km/s and 0.45 km/s for θ = 0° and 90°, respectively.

1. with increasing clustering, a broad peak centered at $v_z = 0$ emerges for photofragment recoil 0° and 90° relative to ε.
2. for cluster photodissociation, the width of the $I_{90}(v_z)$ distribution is narrower than for the $I_0(v_z)$ distribution
3. The width of the calculated curves for the cluster results does not change noticeably from weak cluster to strong cluster conditions.

A velocity dependent anisotropy is calculated from the relation

$$\beta(v) = \frac{I_0(v_z) - I_{90}(v_z)}{\frac{1}{2}I_0(v_z) + I_{90}(v_z)} \tag{3}$$

Because $I_0(v_z)$ and $I_{90}(v_z)$ are well-described by Gaussian functions, $\beta(v_z)$ also has a Gaussian shape, both calculated and observed, as shown in Fig. 2 for 266 and 304-nm photolysis. The 304-nm TOF traces $I_0(v_z)$ and $I_{90}(v_z)$ (not shown in this paper) have a bimodal distribution, which is evident in Fig. 2. For the sake of brevity in this paper, we defer the discussion of this observation to another paper.[13]

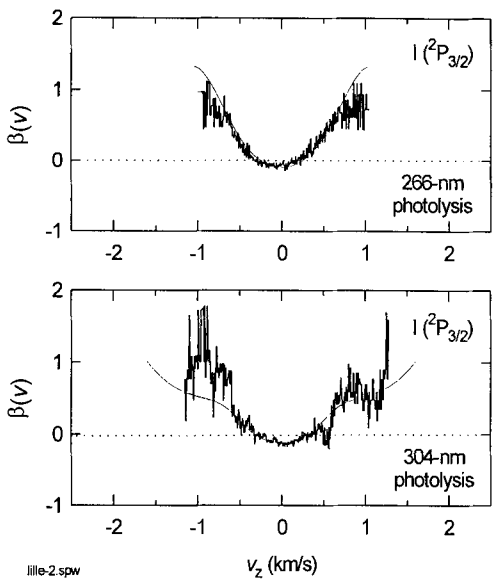

FIG. 2. Velocity dependent anisotropy $\beta(v)$ for $(CH_3I)_n$ cluster excitation at 266 and 304 nm and $I(^2P_{3/2})$ detection. The calculated $\beta(v)$ curves were obtained by substituting the calculated $I_\alpha(v_z)$ curves into Eq. (1).

The c.m. translational energy distribution $P(E)$ for the monomer and cluster photodissociations were evaluated from the $I_0(v_z)$ and $I_{90}(v_z)$. The results for 266-nm photolysis are plotted in Fig. 3. The 304-nm results are presented elsewhere.[13] The $P(E)$ determination in the c.m. frame requires knowing the mass of the counter fragment or, in other words, the parent cluster size. The results presented here are dominated by dimers and to a lesser extent trimers as determined by varying expansion conditions and measuring low-energy electron-impact ionization mass spectra. As it is not possible to ascertain the proportion of the $I_\alpha(v_z)$ that are due to dimers vs. trimers, we evaluate $P(E)$ in Fig. 3 assuming one or the other cluster size in order to place boundaries on the actual translational energy distributions. The velocity dependent anisotropy in Fig. 2 is clearly evident in Fig. 3. Interestingly, $P(E)$ is well described by a Maxwell-Boltzmann distribution despite the anisotropy. The translational energy release, though much less than for the monomer, is still sizable. Assuming dimer conditions, the translational energies correspond to temperatures of 5700 K and 2700 K for $\theta = 0^\circ$ and 90° fragment recoil, respectively.

The anisotropy in the fragment velocity distribution can be understood as a collisional relaxation phenomena. Dissociated I atoms that have undergone few if any collisions in the complex will have an angle-velocity distribution approaching the highly peaked and anisotropic distribution observed for monomer photodissociation. As the residence time and number of collisions in the complex increase, the fragment will lose energy and anisotropy. In the limit of many collisions, one might expect a velocity distribution that is approximately Maxwell-Boltzmann, with the lowest energy fragments being completely isotropic. Loss of I atom anisotropy could be due to residence times in the cluster on the order of a rotational period, or due to angle-deflecting collisions. If the former property is significant, then the translational energy collisional relaxation rate may be determinable from E_t vs t plots, where t is obtained from β by relations for the rotational correlation function. The use of β as a rotational clock for molecules has been demonstrated by Hwang and El-Sayed.[14]

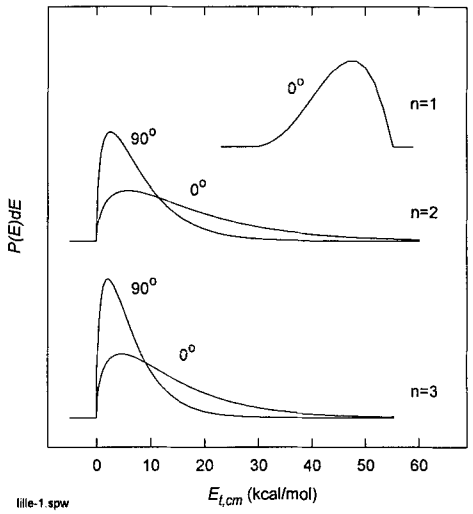

FIG. 3. c.m. translational energy distribution for $(CH_3I)_n$ excitation at 266 nm and $I(^2P_{3/2})$ dissociation. Curves were obtained from the calculated $g(v_z)$ fits to $I_\alpha(v_z)$ in Fig. 1. The n=2 and n=3 results represent how the calculated $P(E_{t,cm})$ are affected by assuming dissociation from dimer vs. trimer. Each curve is normalized to $\int P(E)dE = 1$. The mean translational energies $\langle E_{t,cm} \rangle$ for $\theta = 0^\circ$ and 90°, respectively, are 17.1 and 8.1 kcal/mole assuming n=2, and 13.4 and 6.4 kcal/mol assuming n=3. $\langle E_{t,cm} \rangle$ for n=1 is 45.4 kcal/mol.

The present technique is easily extended to state-specific detection of polyatomic fragments such as CH_3. It is then possible to measure translation, vibration, and rotational energy distributions. The latter two properties are obtained by recording 2+1 REMPI spectra of CH_3 using a medium resolution laser. By measuring the internal energy distribution as a function of fragment velocity and angle, one can determine the anisotropy dependence in these properties, and in principle, the time-dependence for vibrational and rotational relaxation in the manner described above. The use of fragment anisotropy as a clock for fragment residence time in the cluster may not give absolute relaxation rates. However, it should give accurate relative rates of relaxation for translation vs vibration vs rotation under pseudo-condensed-phase conditions. Experimental techniques are not currently available for obtaining this type of information in bulk phase.

REFERENCES

1. J. A. Syage, *J. Phys. Chem.* **99**, 5772 (1995); J. A. Syage, in *Femtosecond Chemistry*, edited by J. Manz and L. Woste (VCH Publishers, New York, 1995), p. 475.; J. A. Syage, in *Ultrafast Spectroscopy in Chemical Systems*, edited by J. D. Simon (Kluwer Academic Press, New York, 1994), p. 289.
2. C. Jouvet and B. Soep, *Chem. Phys. Lett.* **96**, 426 (1983);. C. Jouvet, M. Boivineau, M. C. Duval, and B. Soep, *J. Phys. Chem.* **91**, 5416 (1987).
3. C. Wittig, S. Sharpe, and R. A. Beaudet, *Acc. Chem. Res.* **21**, 341 (1988); S. K. Shin, Y. Chen, S. Nicholaisen, S. W. Sharpe, R. A. Beaudet, and C. Wittig, *Adv. Photochem* **16**, 249 (1991), and references therein.

4. S. I. Ionov, G. A. Bruker, C. Jaques, L. Valachovic, and C. Wittig, *J. Chem. Phys.* **99**, 6553 (1993).
5. N. F. Scherer, L. R. Khundkar, R. B. Bernstein, and A. H. Zewail, *J. Chem. Phys.* **87**, 1451 (1987); N. F. Scherer, C. Sipes, R. B. Bernstein, and A. H. Zewail, *J. Chem. Phys.* **92**, 5239 (1990).
6. J. S. Riley and T. Baer, *Int. J. Mass Spectrom. Ion Proc.* **131**, 295 (1994); K. Ohashi and N. Nishi, *J. Chem. Phys.* **98**, 390 (1993); C. M. Roehl, J. T. Snodgrass, C. A. Deakyne, and M. T. Bowers, *J. Chem. Phys.* **94**, 6546 (1991), and references therein.
7. J. Segall, Y. Wen, R. Singer, C. Wittig, A. Garcia-Vela, and R. B. Gerber, *Chem. Phys. Lett.* **207**, 504 (1993); C. Jaques, L. Valachovic, S. Ionov, E. Bohmer, Y. Wen, J. Segall, and C. Wittig, *J. Chem. Soc. Faraday Trans.* **89**, 1419 (1993).
8. R. J. Bemish, E. J. Bohac, M. Wu, and R. E. Miller, *J. Chem. Phys.* **101**, 9457 (1994).
9. R. Ogorzalek Loo, G. E. Hall, H.-P. Haerri, and P. L. Houston, *J. Phys. Chem.* **92**, 5 (1988).
10. S. M. Penn, C. C. Hayden, K. J. Carlson Muyskens, and F. F. Crim, *J. Chem. Phys.* **89**, 2909 (1988).
11. M. A. Young, *J. Chem. Phys.*, in press (1995); M. A. Young, *J. Phys. Chem.* **98**, 7790 (1994).
12. R. A. Hertz and J. A. Syage, *J. Chem. Phys.* **100**, 9265 (1994).
13. J. A. Syage, *Chem. Phys. Lett.*, submitted; J. A. Syage, *Chem. Phys.*, submitted.
14. H. J. Hwang and M. A. El-Sayed, *J. Chem. Phys.* **94**, 4877 (1991); H. J. Hwang and M. A. El-Sayed, *J. Chem. Phys.* **96**, 856 (1992).